Chapter-II

Almond oil based multifunctional greener additives for lubricating oil

2.2.1 Introduction

Lubricating oils are principally a blend of a base oil and an additive, mixed in different ratios according to the requirements for various purposes.[1] The additives normally boost the rheological properties of the lubricant base oils,[2] such as variation of its viscosity with temperature (viscosity index, VI),[3] low temperature flow ability (pour point, PP),[4] together with optimising other parameters to a satisfactory level. Although additives of numerous types have been devised to optimize the modern lubricants, acrylate based polymers are in use as an additive for quite a long time.[5]

The base oil of the lubricating oils is typically derived from petroleum and principally consists of a mixture of paraffinic hydrocarbons of different chain lengths. However, these crude oil wells are exhausting very fast and, thus, so are the main reserves of lubricating oils.[6] These oils and additives also pose a potential risk to the ecology due to their inherent non-biodegradability and their role in water and soil contamination, caused by spillage during application or improper disposal of the used oil. Stringent regulations are, therefore, currently being imposed in a number of countries on mineral oil-based lubricants together with their non-biocompatible toxic wastes supplies.[7,8] This increasing ecological consciousness, together with the challenge to develop lubricants with characteristics superior to those based on mineral oil only has provided researchers with the momentum to search for some novel, environmentally benign, multifunctional additives. In this search, vegetable oils have been considered as a potential candidate. Vegetable oils are oils that have been extracted from various plants. They are largely triglycerides of long chain fatty acids. Multidisciplinary research efforts have yielded a high level of technical and commercial success with respect to these bio-based materials.

These plant oils are currently in the focus of the chemical and polymer industry, as they have many useful properties including natural biodegradability,[9,10] good lubricity, non toxicity, high viscosity index,[11] low cost and various other excellent tribological properties.[12-14] They also present the largest renewable platform due to their universal wide availability and sustainability. Different vegetable oils, such as sunflower oil, soybean oil, garlic oil, etc. are currently being looked as a potential replacement for petroleum based lubricating oils and synthetic esters (modified petroleum based components for specific uses).[15,16] However, extensive application of these bio-oils is still challenged by one or more of their possible inherent limitations. The fatty acid chains of almost every vegetable oil have a high degree of C–C unsaturations, resulting in poor thermal and oxidative stability and limiting their use as lubricants to a narrow range of temperature.[17] These oils also experience poor low temperature fluidity which leads to degradation, rapid thickening and deposit formation of the oil at low temperature.[18,19] Hence, plant oils must be genetically or chemically customized to improve their desired properties. This can be attained by homopolymerisation of the oil or its copolymerisation with an appropriate monomer.[15] The introduction of a second type of monomer unit in the polymer moiety of the oil may introduce some additional properties and features to the copolymer.

Hence, with a view of developing novel, environmentally benign, polymeric additives for lubricating oil and with features better than petroleum oils, the author chose almond oil (AO). Almond oil, being a good source of naturally derived unsaturated fatty acids,[20] is a suitable candidate to incorporate biodegradability in its acrylate copolymer.

2.2.2 Experimental section

2.2.2.1 Materials

Almond oil (AO) was collected from a local grocer's shop. Acrylic acid (stabilized with 0.02% hydroquinone mono methylether) was obtained from Sisco Research Laboratories Pvt. Ltd., (India). Toluene was from Merck Specialties Pvt. Ltd., (India). Methanol (Thomas Baker Chemicals Pvt. Ltd., India) and decanol (Loba Chemie Pvt. Ltd., India) were used as-received. Before use, AIBN (Azobisisobutyronitrile, Spectrochem Pvt. Ltd., India) was recrystallized from $CHCl_3$–CH_3OH. Mineral base oils (BO1 and BO2) were received from Indian Oil Corporation Ltd. (IOCL), India. The physical properties of the base oils are tabulated in Table 2.2.1. Fungal specimens for testing the biodegradability of the polymers were obtained from the Department of Microbiology, North Bengal University, West Bengal, India.

2.2.2.2 Esterification of acrylic acid with decyl alcohol

The ester, decyl acrylate (DA), was prepared by reacting 1 mol of decyl alcohol with 1.1 mol of acrylic acid. The reaction was carried out in a three necked round bottom flask in 100 mL of toluene and 0.25% of hydroquinone with respect to the reactants as polymerization inhibitor and under a slow stream of deoxygenated nitrogen. Conc. H_2SO_4 was used here as a catalyst.

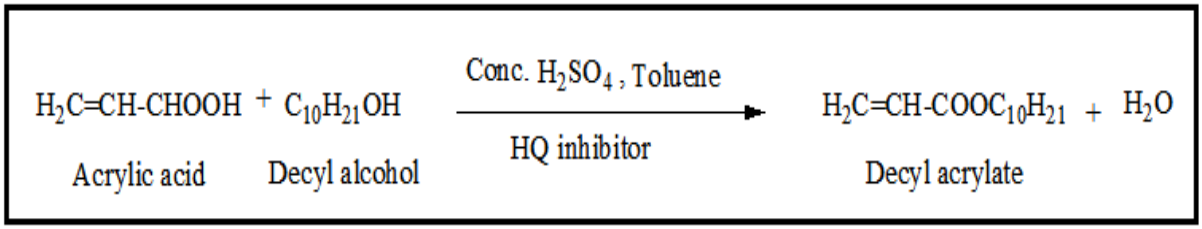

Scheme 4: Preparation of the ester decyl acrylate

The reactants were thoroughly mixed in toluene and were heated slowly from room temperature to 403 K using a thermostat and a Dean–Stark apparatus for water separation. The amount of water liberated helped in monitoring the extent of reaction.

2.2.2.3 Purification of the decyl acrylate ester

For the purification of decyl acrylate ester, 1 g of charcoal was added to it and refluxed for 3 hours. After the stipulated time, the charcoal was filtered off and the filtrate was washed in a separation funnel with 0.5N NaOH. To ensure the complete removal of any unreacted acids, the process was repeated a number of times. The ester was then rinsed a number of times with distilled water to eliminate any NaOH (if present in small amount) until it became neutral to pH paper. The ester DA was finally left over night on anhydrous $CaCl_2$ for drying. The $CaCl_2$ was then removed by filtration and toluene was recovered by distillation under reduced pressure.[5] The ester left behind was ready for further use.

2.2.2.4 Synthesis of the polymer

The homopolymerization of AO and its copolymerization with decyl acrylate were carried out in a four necked, round-bottom flask. The homopolymer of AO (HAO) was prepared by taking 10 g of AO in the round-bottom flask equipped with a thermometer, mechanical stirrer, condenser and an inlet for the introduction of nitrogen. AIBN (0.4% of the monomers) was used as an initiator and was added in five different lots during the reaction. The reaction was carried out for 7 h and the temperature was maintained at 363 K to prepare the homopolymer. The reaction mixture was poured into methanol,

at the end of the reaction time, with stirring, to terminate the polymerization and precipitate the polymer. Additional purification of HAO was carried out by repeated precipitation of its hexane solutions by methanol followed by drying under vacuum at 313 K. Similar synthesis was carried out for preparation of the copolymers by taking 10 g total of AO with 5 or 10% of DA, keeping the other components the same. The mass fraction of the monomers in the copolymers is given in Table 2.2.2.

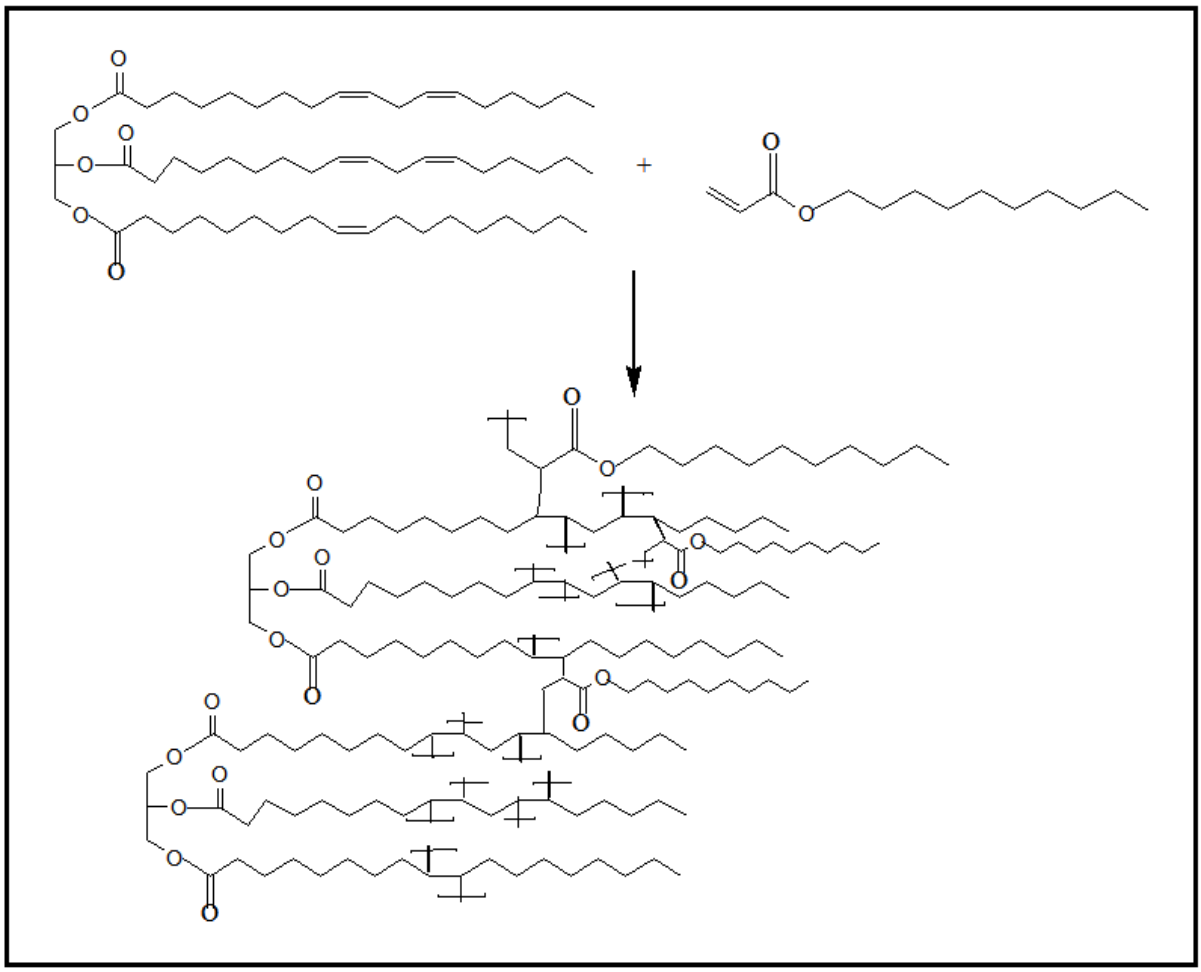

Scheme 5: Preparation of copolymer of almond oil with decyl acrylate

2.2.3 Measurements

2.2.3.1 Spectroscopic measurements

NMR spectra were recorded in an Avance 300 MHz FT-NMR instrument (Bruker Corporation, Germany) using a 5 mm BBO probe. Tetramethylsilane (TMS) was used here as reference material and $CDCl_3$ as a solvent. The IR spectra were recorded on a FT-IR 8300 spectrometer (Shimadzu Corporation, Japan) using 0.1 mm KBr cells at room temperature, within the wavenumber range of 400–4000 cm^{-1}.

2.2.3.2 Thermo gravimetric measurements

The thermal stabilities of all the prepared polymers (additives) were determined by a TGA-50 thermogravimetric analyzer (Shimadzu Corporation, Japan), at a heating rate of 10 °C/min using an alumina crucible. The thermo-oxidative stability of the additives was determined in terms of percent of weight loss (PWL) with increase in temperature. A higher decomposition temperature for the polymer for a given PWL indicates a superior thermo-oxidative stability. The PWL was determined by the equation,

$$PWL = [(M_0 - M_1)/M_0] \times 100 \qquad \text{Eq. (1)}$$

where M_0 is the initial mass and M_1 is the left over mass of the polymer until constant weight, after the test.

2.2.3.3 Determination of molecular weight of the prepared polymers

The molecular weights of the prepared polymers were determined using a GPC system (Waters Corporation, USA) equipped with a 2414 refractive index detector (polystyrene calibration), a 717 plus autosampler and a Waters 515 HPLC pump (Table 2.2.3). HPLC grade THF was used as an eluent at a flow rate of 1.0 mL/min at 30 °C. The

polydispersity index (PDI, M_w/M_n) of the prepared polymers (which indicates the nature of distribution of the molecular weights in the prepared polymers) was calculated by determining the weight-average molecular weight (M_w) and number-average molecular weight (M_n) of the polymers.

2.2.3.4 Evaluation of viscosity index (VI)

The viscosity index (VI) is a parameter that indicates the effect of alteration of temperature on the kinematic viscosity (KV) of the oil. A higher value of VI denotes a lower rate of change of viscosity with the variation in temperature. The viscosity index was calculated as per the ASTM D2270 method for the two base oils (BO1 and BO2) [21]. The KV of the base oils blended with the additives was evaluated at 313 and 373 K, at different concentrations of the additive, to analyse the effect of concentration on VI of the additive mixed lube oil. KV was calculated by the equation,

$$KV = (Kt - L/t)\,\rho \qquad \text{Eq. (2)}$$

where K and L are viscometric constants; ρ is the density of the additive mixed oil and t is the time of flow of the additive mixed base oil to pass through the two calibrated marks in the Ubbelohde viscometer.

2.2.3.5 Evaluation of the pour point (PP)

The pour points of the two lube oils (BO1 and BO2) with added synthesised additives were evaluated according to the ASTM D97-09 method on a cloud and pour point tester (Wadegati Labequip Pvt. Ltd., India). The result of additive concentration on the PP was analysed by using different concentrations of the additives.

2.2.3.6 Biodegradability test

Numerous tests have been devised for assessing the biodegradability of plant oil based additives, as they have an innate biodegradability compared to the synthetic acrylate ones. Here the biodegradability was evaluated by (a) the soil burial degradation test of films of the additives as per ISO 846:1997[22,23] and (b) the disc diffusion method against fungal pathogens.[24] The degree of degradation of the additives in the experiments was assessed by calculating the percent weight loss (PWL) of the samples. The degradation of the additives was also affirmed by examining the shift in the IR frequency of the ester carbonyls along with the change in their molecular mass after the biodegradability test.

2.2.3.6.1 Soil burial degradation test (SBD Test)

The effect of microorganisms on the surface of polymer film is studied in the SBD test.[25] Here, 2 g of every polymeric additive was taken to produce the polymer films. The films so created were then buried in soil in a bacteriological incubator. The soil (containing the microorganisms) was first placed in a tray, its relative humidity was set to 50–60% by adjusting the humidity chamber and the temperature was selected at 303 K. The soil for this work had been gathered from the North Bengal University campus (West Bengal, India) with pH 7.3 and moisture of 25%. The buried polymer films were taken out for study up to a period of 3 months at regular intervals of 15 days. For each work (time interval), a different film was used. Recovered films after the biodegradation test were washed with chloroform, filtered with Whatman grade 41 filtration paper and dried in a vacuum oven at 323 K. They were then again decontaminated by precipitation

of their hexane solution by methanol and then dried in a vacuum oven until a constant weight was reached at 323 K. The weights of the sample, before and after drying, were recorded to determine the PWL.

2.2.3.6.2 *Disc diffusion (DD) method*

In this test method, four fungal pathogens, viz. *Colletotrichum gloeosporioides* (CG), *Fusarium equiseti* (FE), *Colletotrichum camelliae* (CC) and *Alternaria alternate* (AA) were selected to check the biodegradation of the prepared samples in a bacteriological incubator (Sigma Scientific Instruments Pvt. Ltd., India). Culture media for the fungal strains were first prepared by mixing potato extract, agar powder and dextrose in a 10:1:1 proportion by mass. 3 g of the culture media was taken in Petri dishes with 2 g of each of the additives and incubated for 30 days at 310 K with the selected fungal pathogens. A change in colour from yellow to blackish was indicative of the fungal growth. After 30 days, the polymeric additives were recovered from the fungal strains and washed with chloroform, purified and then dried. The PWL [Eq. (1)] for each of the samples was recorded and their molecular weights were determined by GPC method.

2.2.4 Results and discussion

2.2.4.1 Spectroscopic analysis

The FT-IR absorption indicated the presence of ester carbonyl groups of HAO at 1744.4 cm^{-1}. The broad peak in the region of 1165.7 cm^{-1} was due to the ester C–O stretching vibration. The peaks emerging in the regions of 723.9, 1377.8 and 1463.8 cm^{-1} corresponds to the C–H bending vibrations of CH_2 and CH_3 groups. Absorptions

appearing in the regions of 2855.1 cm^{-1} and at 2926.1 cm^{-1} were due to the stretching vibrations of the paraffinic C–H bonds. The nonexistence of olefinic peaks in the range of 1550–1680 cm^{-1} in the polymer and their appearance in the monomers supports the polymer formation (Fig. 2.2.1).

In the ^{1}H-NMR spectra of HAO (Fig. 2.2.3), the triglyceride group protons (–$COOCH_2$) showed broad peaks in the range of 4.1–4.3 ppm. Peaks also emerged for the methylene protons in the range of 1.3–2.2 ppm while the peaks in the range of 0.86–0.88 ppm were for the methyl protons. The shift between 2.3 and 2.4 ppm occurred due to the protons of –$OCOCH_2$– groups present in HAO. The nonappearance of any peaks in the range of 5.5–6.5 ppm also supports the formation of the polymer.

In the proton decoupled ^{13}C-NMR spectra of HAO (Fig. 2.2.5), the methyl and methylene carbon atoms of AO showed signals between 14.1 and 33.9 ppm. The signals appearing between 172.9 and 178.5 ppm is attributed to the carbonyl carbons of the ester groups whereas the –OCH_2 carbons of the triester appeared between 62.1 and 68.9 ppm. The absence of unsaturation in the polymers was indicated by the lack of any peaks in the range 130–150 ppm.

Polymers S-2 and S-3 showed related peaks in their NMR (^{1}H and ^{13}C) and FT-IR spectrum suggesting that the prepared polymers are in good agreement with the expected structures.

2.2.4.2 Thermogravimetric analysis (TGA) study

The studies of the thermogravimetric analysis of the polymers are shown in Table 2.2.4. Here, two different decomposition temperatures of the polymers are reported for a better comparison. The polymer S-1 at 300 °C showed a PWL value of 52 while at 425

°C it had a PWL of 94. The polymer S-2 for a similar PWL (values of 49 and 93) has a higher decomposition temperature of 325 and 465 °C respectively. As indicated by the percentage of degradation (measured in terms of PWL) of the polymers, it is quite clear that the thermal stability of the copolymers was moderately superior to that of the homopolymer. Additionally, it was also learned that the copolymer S-3 is more stable at higher temperatures compared to the other polymers with the highest decomposition temperature of 360 and 490 °C for the PWL values of 48 and 95 respectively. This increased stability is may be due to a lower level of branching in the copolymer S-3 as suggested by the respective PDI values in Table 2.2.3.[26]

2.2.4.3 Performance of the prepared additives as viscosity index improvers

The VI values of the lube oils blended with the additives are shown in Figs. 2.2.8 and 2.2.9. Detailed study of the data as obtained showed that the VI values of the base oils were significantly augmented by the addition of the additives. Besides, the result improved with the increase in additive concentration regardless of the additive and the base oil used. A critical examination of the VI values also explained that the copolymers acted as a better VI enhancer in contrast to the homopolymer. The inclusion of DA in the almond oil backbone improved the VI values and the improvement was highest for the copolymer S-3 with a greater proportion of DA, followed by copolymer S-2, and then the polymer S-1. Here, the increase in the VI results with growing additive concentration in the lube oil can be the outcome of increased hydrodynamic volume of the additive. Hydrodynamic volume is the volume of the polymer and the associated base oil. The potential of a polymer to operate as a VII is directly associated with the hydrodynamic volume occupied by the randomly coiled polymer chain.[27] It is claimed that in cold

conditions the polymers have a small hydrodynamic volume i.e., the molecules of the polymer take up a coiled form so that their influence on viscosity is minimized. At elevated temperature, when the viscosity of the lube oil is likely to decrease, an expansion or uncoiling of the polymer molecules takes place ensuring an increase in the size of the polymer micelle. This inflated micelle, simultaneously with the increase in the power of solvation at higher temperature, nullifies the drop in viscosity of the base oil with increase in temperature.[28] Hence, higher the proportion of polymer in the base oil, bigger is the volume of the micelle and subsequently higher will be the viscosity index.[29]

2.2.4.4 Performance of the prepared additives as pour point depressants

Assessment of the synthesised additives for their PPD properties showed good results (Figs. 2.2.10 and 2.2.11). It is clearly noticeable that the effectiveness of the prepared polymers as PPDs steadily improved with their increasing concentration in the base oils studied. Also the results suggested that the prepared additive sample S-3 was more effective as a PPD than the homopolymer (S-1) and the other copolymer (S-2) with different acrylate ratio in the base oils. The dissolved wax like paraffinic hydrocarbons present in mineral oils have a tendency to separate from the oil at low temperatures appearing as a stiff network of crystals which checks the oil from flowing.[30] With the purpose of improving its pour point (the lowest temperature at which the oil stays flowing), pour point depressants are suitably blended to the oil. The blending of additives disrupts these stiff networks of wax crystals preventing their formation. Different theories have been proposed for the mode of action of PPDs, among which nucleation, co-crystallization, adsorption and improved wax solubility are

generally accepted.[31,32] The PPD molecules usually consists of a wax like paraffinic part that works by offering nucleation sites and co-crystallizes with the mineral oil's wax like hydrocarbons and gradually become a part of them while the polar segments associated with the PPDs, dissimilar to the wax crystals, prevents the expansion of the rigid network of wax matrices.[33] The almond-acrylate copolymers, owing to their more polar behaviour,[33] are more valuable against the creation of wax crystals, thereby claiming superior pour point results compared to that for the homopolymer.

2.2.4.5 Photo micrographic analysis

A BPL-400B polarizing microscope (Banbros Engineering Pvt. Ltd., India) was selected to study the photomicrographs of the additive blended base oils (Fig. 2.2.12). The photomicrographs depicted the wax crystallization response of the synthesised polymers dissolved in the base oils. The temperature of the oils for analysing the photomicrographs was controlled on the microscope slide by an attached cooling thermostat. The magnification of the microscope was adjusted at ×200 and all photos were taken at 273 K. The photomicrographs explained that the wax morphology changed in accordance with the nature of additives added. Fig. 2.2.12a, which is for the pure lube oil, has large wax crystals of estimated 100 μm size; on doping with the additives there was a substantial reduction of wax crystal dimension along with the formation of several highly dispersed small crystals. The polymer S-3 (Fig. 2.2.12d) has the smallest dispersed wax crystals compared to the others. These results are in conformity with the pour point values obtained earlier.

2.2.4.6 Analysis of biodegradability test

Weight losses of the additive samples after the SBD and DD biodegradability tests are reported in Fig. 2.2.13 and Table 2.2.5 respectively. The analysis of the investigations showed considerable biodegradation for all the additives. The results of the SBD tests pointed out that the biodegradation of the additives under study increased continuously with the increasing number of days. Additionally, all the polymers of almond oil had notable weight losses against the fungal pathogens, especially against *Alternaria alternate* (AA), in the DD test. The GPC of the polymers after the DD method was also carried out and the results were compared with the respective polymers before biodegradation. The results indicated considerable change in the M_n and M_w of the polymers and thus revealed the biodegradability of the prepared polymers. Furthermore, as expected for zero acrylate percentage and owing to the presence of the bio-based monomer unit, the additive S-1 displayed the highest biodegradability in comparison to all the additives in both of the tests. The FT-IR spectra of the HAO additive, before and after the DD test (Fig. 2.2.7), were also compared. The IR peaks of the additive S-1 at 1744, 1464, 1378, 1166 and 724 cm^{-1} diminished noticeably in peak height and intensity after the DD test. This decrease in the IR peak intensities is possibly due to the scission of the polymer chains during biodegradation of the polymer units.[34] The other additives also displayed shift in their IR peaks but to a much smaller extent. The drop and the shift in the IR peak intensities of the additives after the biodegradation tests along with the results of PWL of the additives confirmed the biodegradable nature of the synthesised additives.

2.2.5 Conclusions

The above findings pointed out that all the prepared additives worked as excellent multifunctional additives augmenting the lubricant property of the base oils. Some key improvement in pour point and viscosity index values were obtained by the inclusion of acrylate monomers in the triglyceride backbone of the almond oil. The thermal stability of almond oil increased significantly with polymerization. Again, the thermo-oxidative stability of the copolymer with highest DA content was the maximum and had the best performance. The VI values, as obtained, improved with the increase in the proportion of the additives, and polymer S-3, with a higher fraction of DA, worked as a superior VI improver compared to the others. Furthermore, it was also found that the copolymer S-3 operated more efficiently as a PPD than the homopolymer for the given lube oils under investigation. The biocompatible natures of the additives were also recognized and HAO displayed the highest biodegradability among the prepared additives. Hence, we suggest that the prepared additives may be used for the formulation of a biodegradable, multifunctional additive for lube oils for a greener future.

2.2.6 References

References are given in BIBLIOGRAPHY under Chapter-II of Part-II (Page No. 214-218).

2.2.7 Tables and figures

Table 2.2.1: Physical properties of base oils

Properties	***Method***	***BO1***	***BO2***
Viscosity at 40 °C in cSt	ASTM D445	7.132	23.387
Viscosity at 100 °C in cSt	ASTM D445	1.849	3.911
Viscosity Index	ASTM D2270	80	85
Pour Point, °C	ASTM D97	-3	-6
Density ($g.cm^{-3}$) at 40 °C	ASTM D4052	0.83645	0.85492

Table 2.2.2: Percentage composition of the copolymers as estimated by spectroscopic method

Polymers	***Mass fraction in the polymers***		***NMR estimation of the mass fraction of decyl acylate***	***IR estimation of the mass fraction of decyl acylate***
	Almond oil	***Decyl acrylate***		
S-1	1	0	-	-
S-2	0.95	0.05	0.020	0.023
S-3	0.90	0.10	0.041	0.048

S-1: Homopolymer of almond oil, S-2: almond oil + 5% decyl acrylate, S-3: almond oil + 10% decyl acrylate.

Table 2.2.3: Average molecular weight and PDI values determined by GPC

Polymers	$M_n \times 10^4$	$M_w \times 10^4$	***PDI***
S-1	2.157	3.301	1.53
S-2	1.989	2.766	1.39
S-3	1.782	2.458	1.37

Table 2.2.4: TGA data of the polymer samples

Polymers	***Decomposition temperature (°C)***	***PWL***
S-1	300/425	52/94
S-2	325/465	49/93
S-3	360/490	48/95

Table 2.2.5: Result of biodegradability test by DD method and comparative average molecular weight values

Polymers	*Incubation period (days)*	*Pathogen*	*PWL*	*Molecular weight*			
				Before biodegradation		*After biodegradation*	
				M_w	M_n	M_w	M_n
S-1	30	CC FE AA CG	0.35 0.73 26.28 0.79	33018	21575	29249	20312
S-2	30	CC FE AA CG	0.21 0.51 16.72 0.48	27669	19897	25308	18756
S-3	30	CC FE AA CG	0.11 0.34 12.09 0.36	24588	17824	22286	16772

Figure 2.2.1: IR spectra of polymer S-1

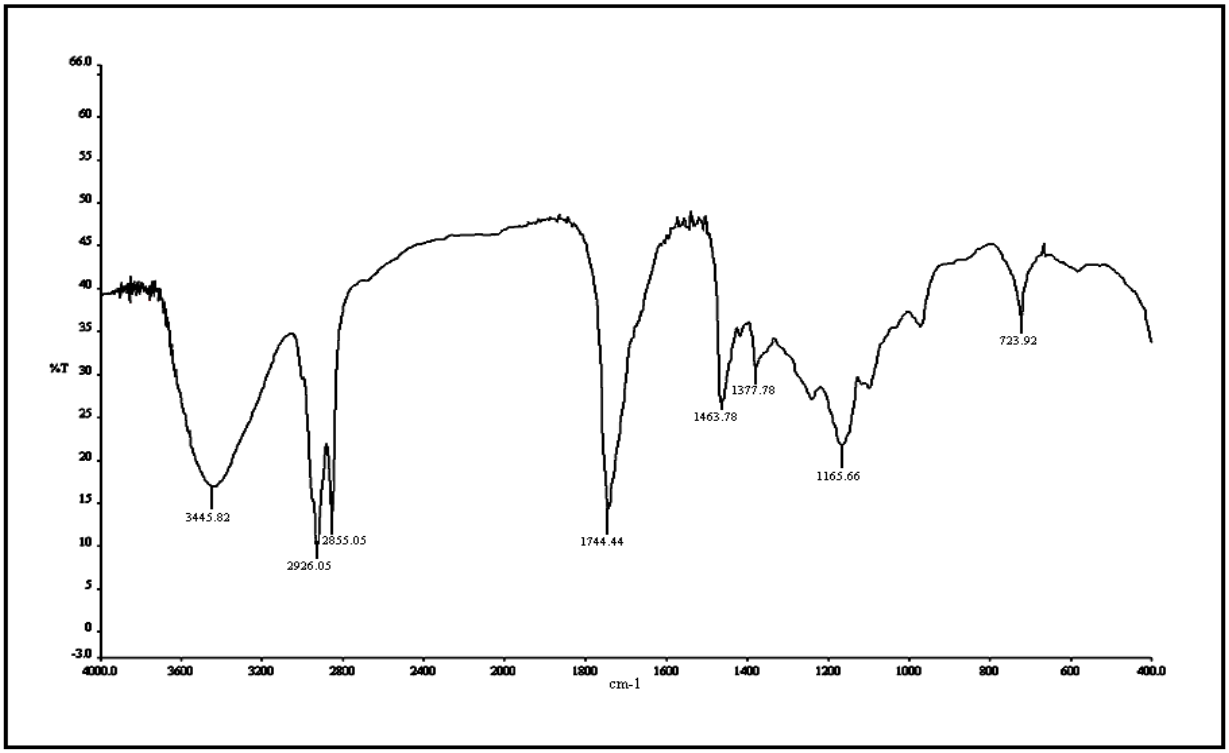

Figure 2.2.2: IR spectra of polymer S-2

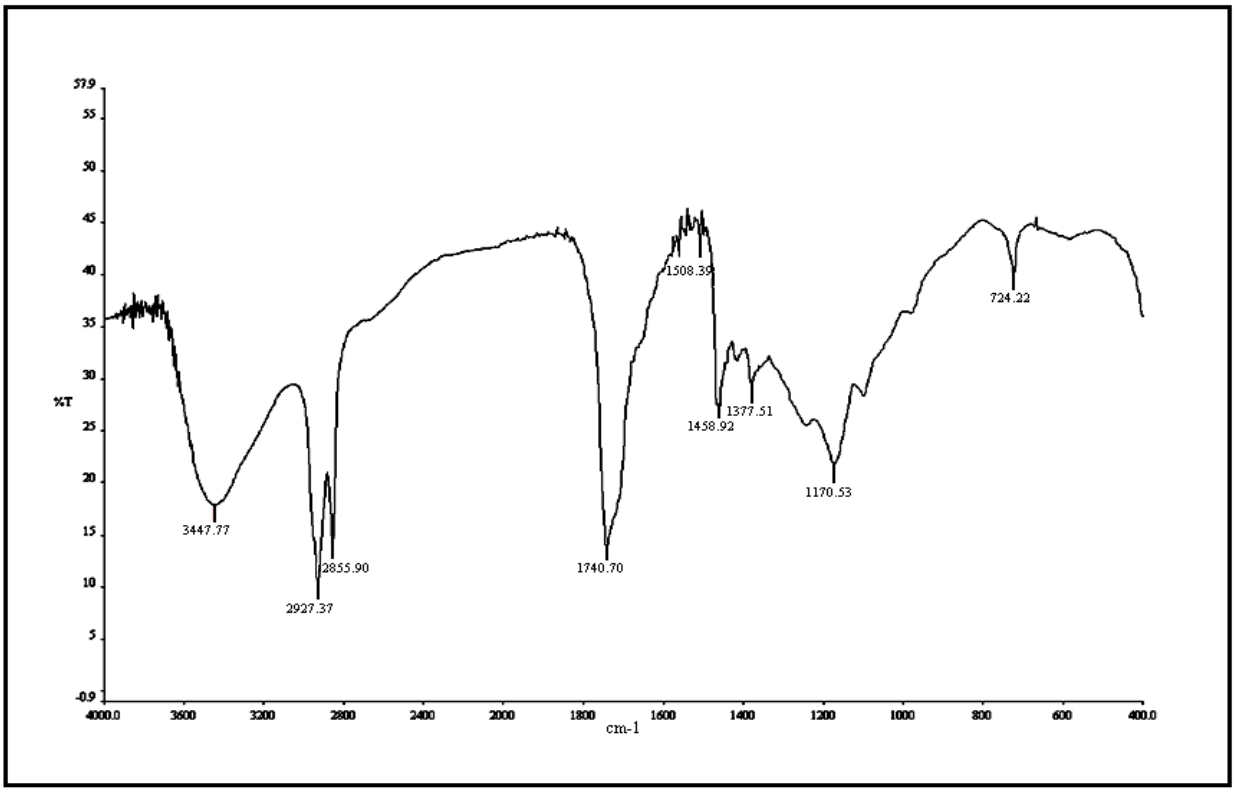

Figure 2.2.3: ^{1}H-NMR spectra of polymer S-1

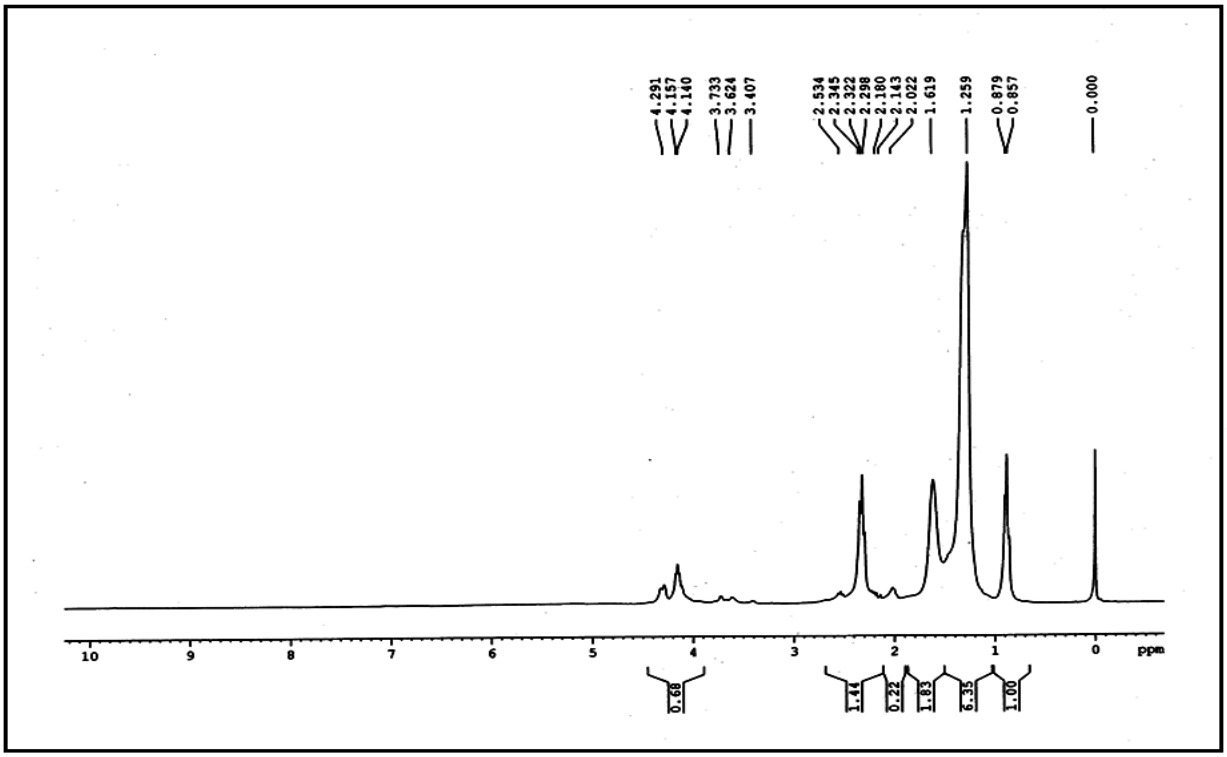

Figure 2.2.4: ^{1}H-NMR spectra of polymer S-2

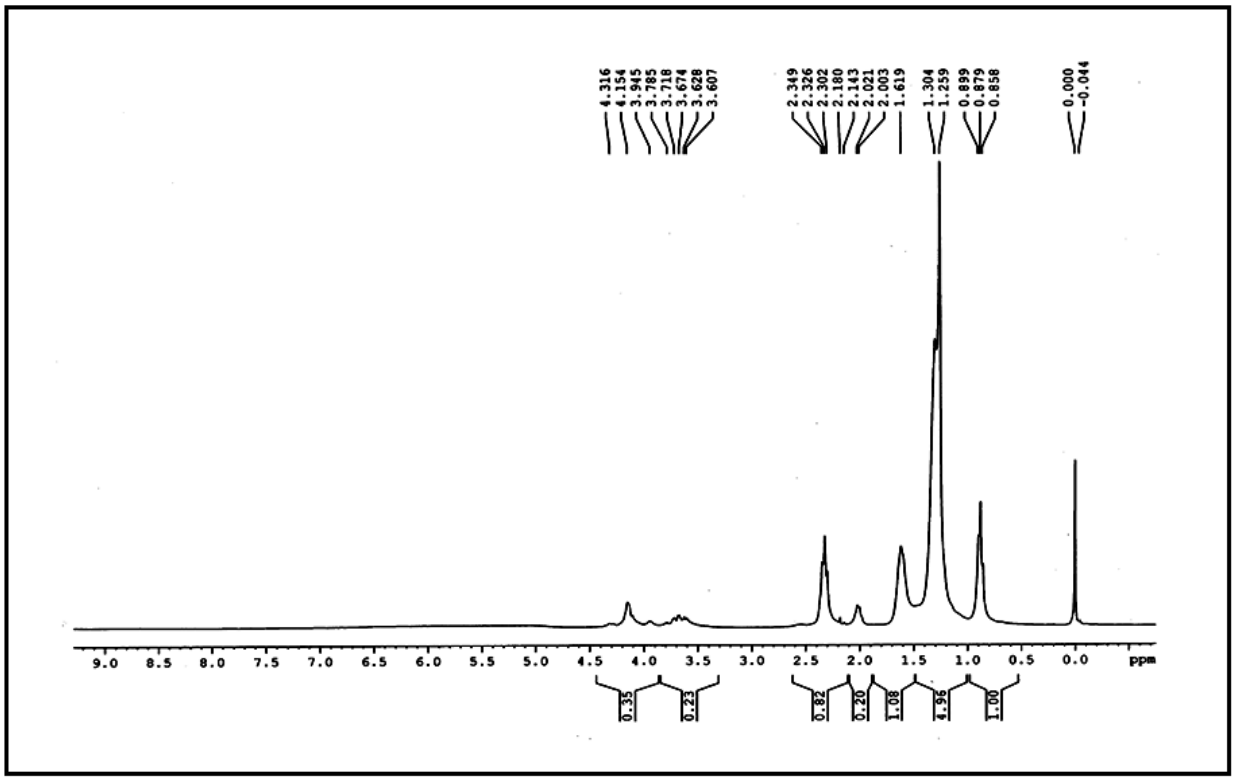

Figure 2.2.5: ^{13}C-NMR spectra of polymer S-1

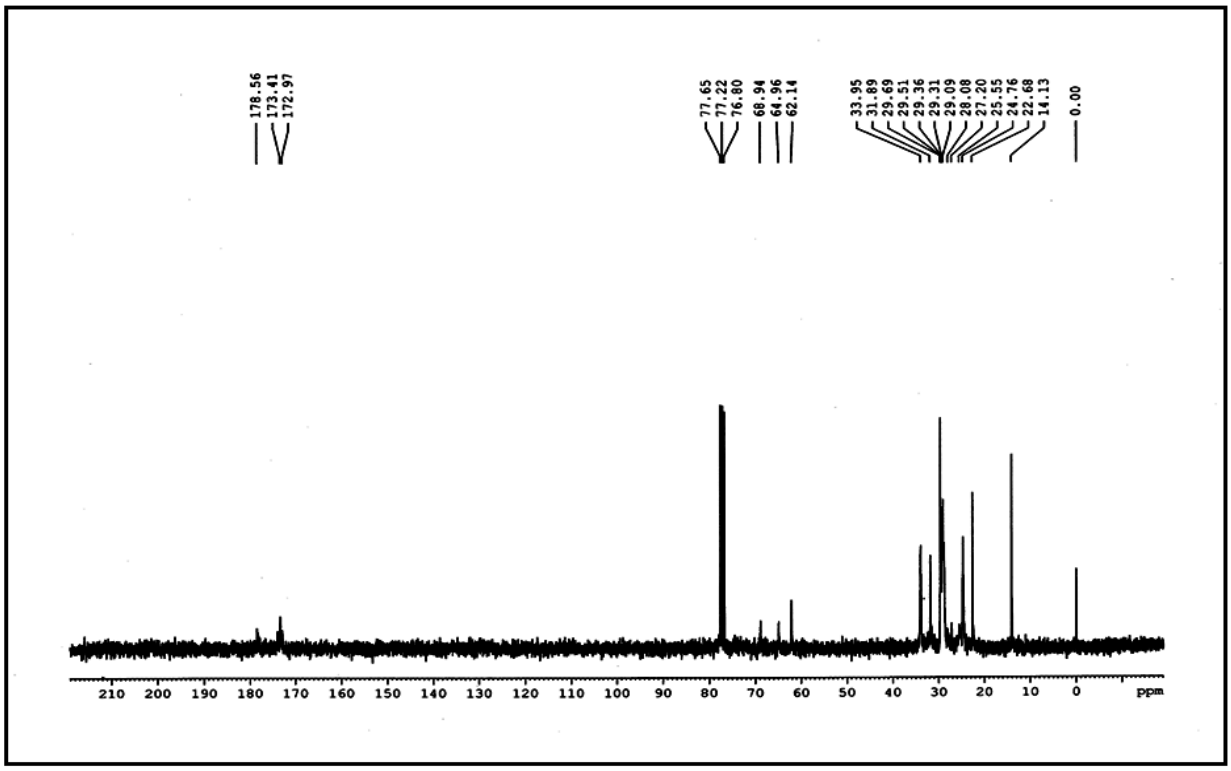

Figure 2.2.6: ^{13}C-NMR spectra of polymer S-2

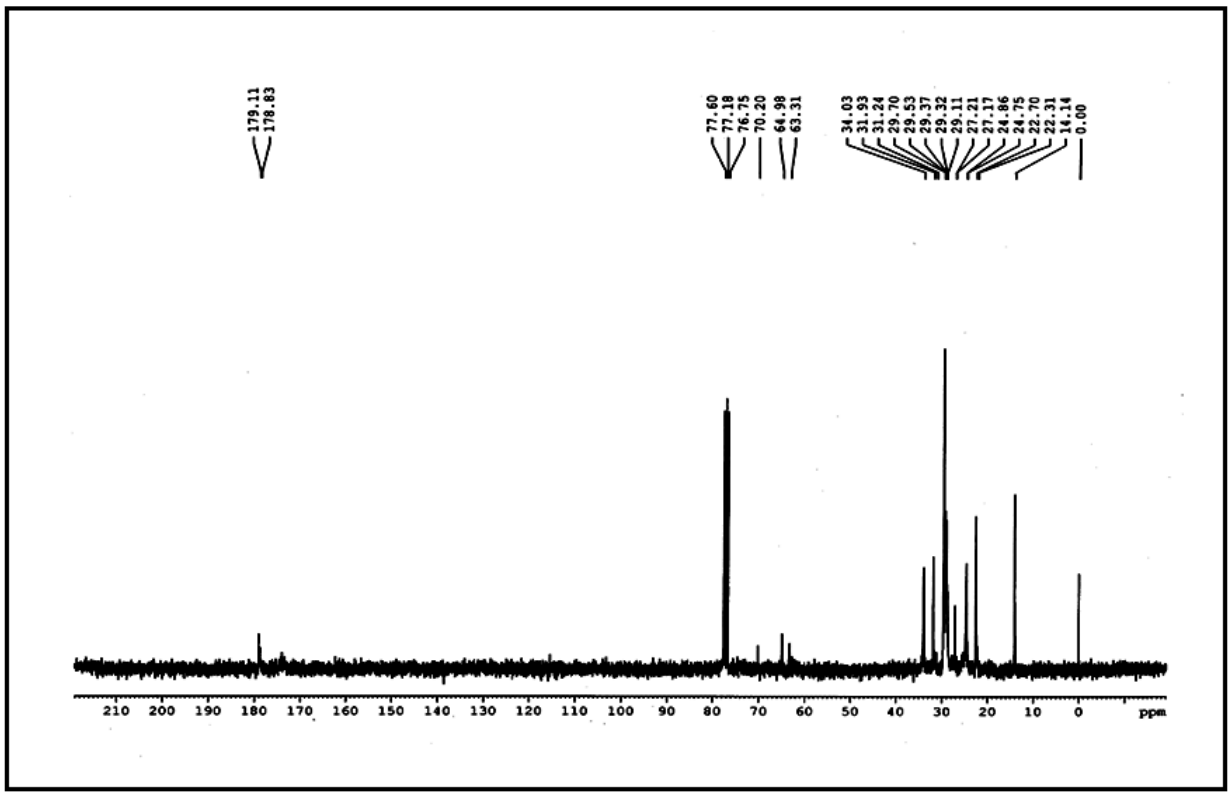

Figure 2.2.7: Comparative FT-IR spectra of polymer S-1 (a) before and (b) after the DD test

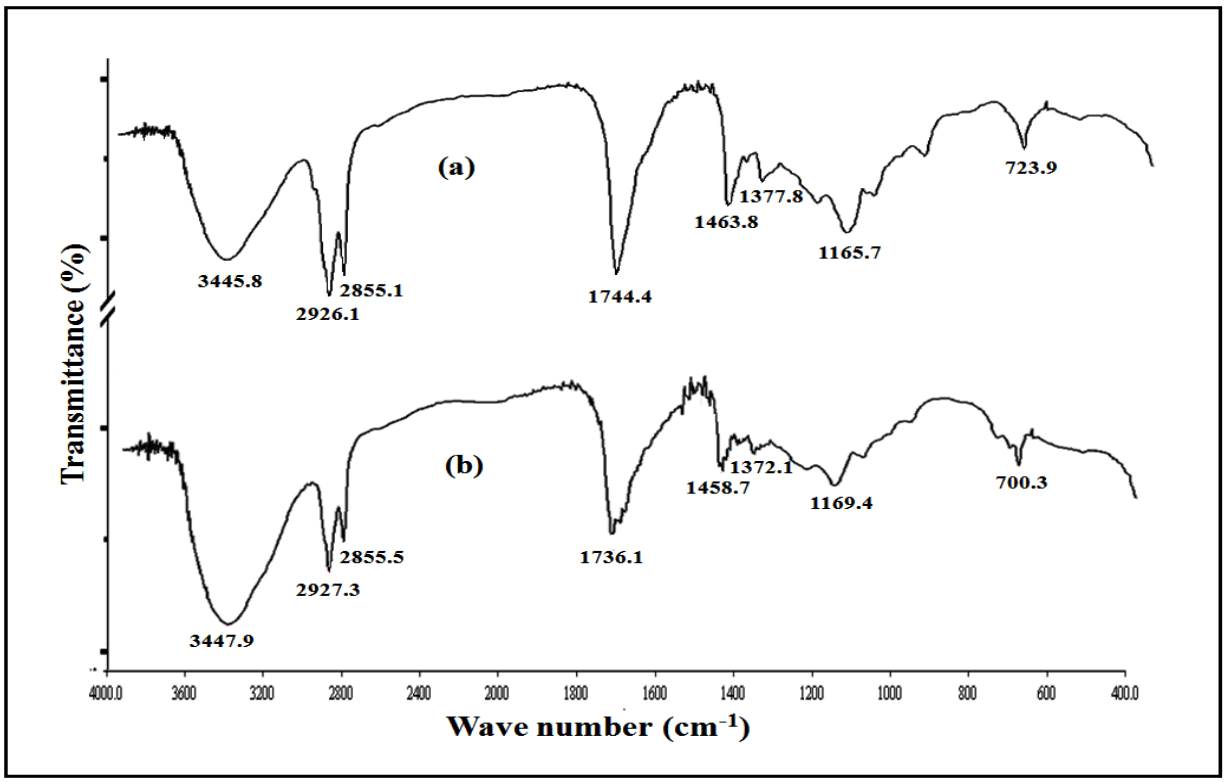

Figure 2.2.8: Viscosity index values of additives S-1 to S-3 doped in base oil BO1

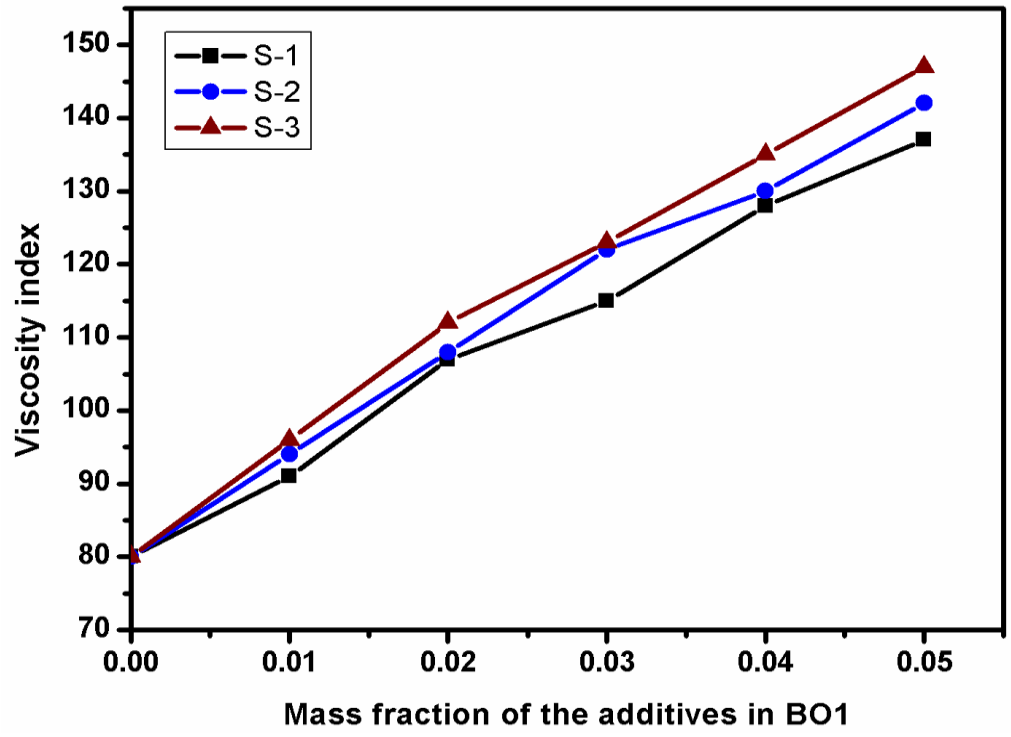

Figure 2.2.9: Viscosity index values of additives S-1 to S-3 doped in base oil BO2

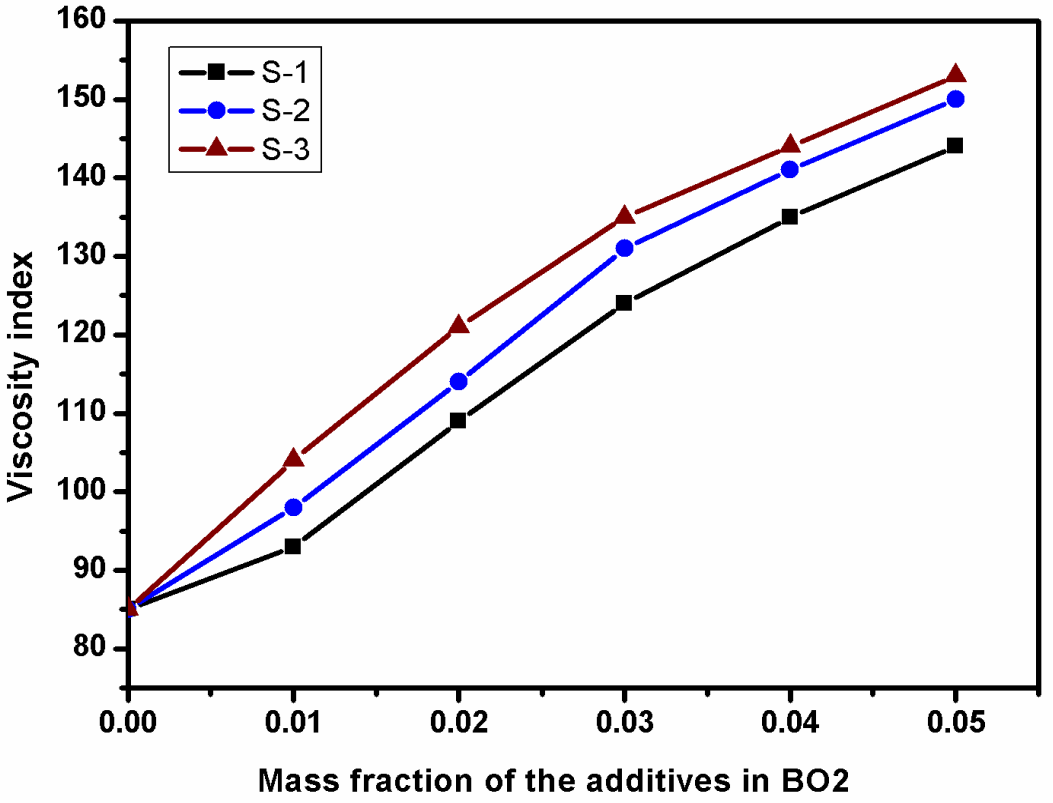

Figure 2.2.10: Pour point of the additives S-1 to S-3 doped in base oil BO1

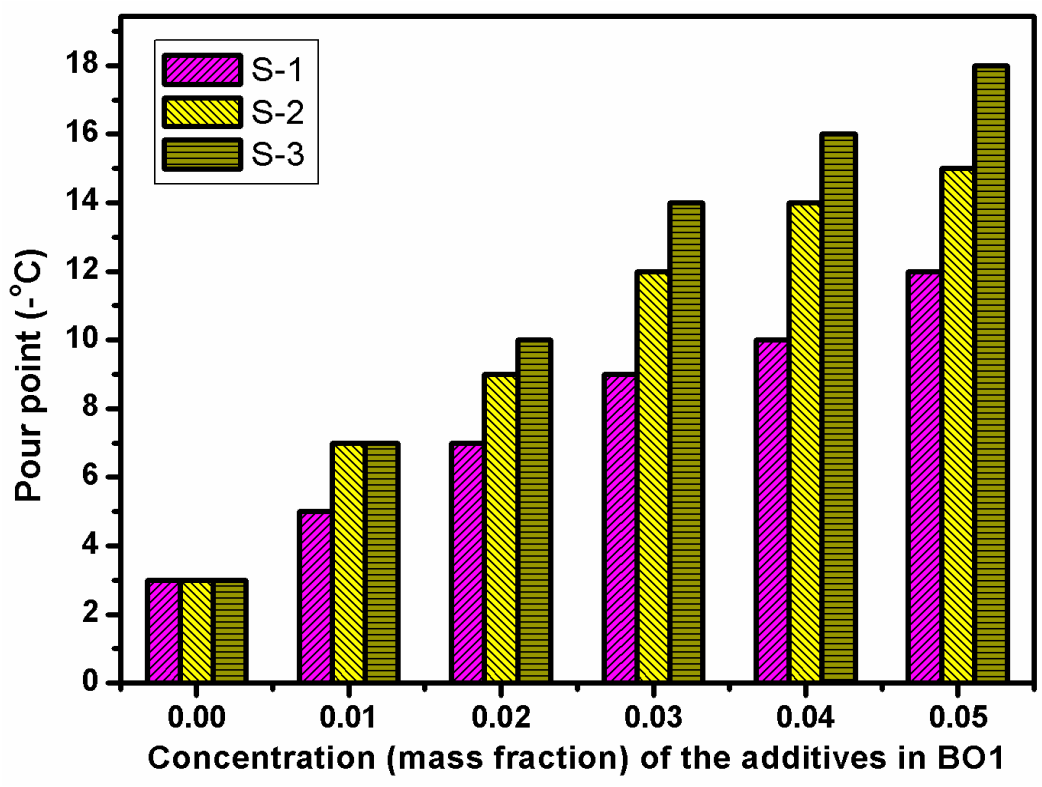

Figure 2.2.11: Pour point of the additives S-1 to S-3 doped in base oil BO2

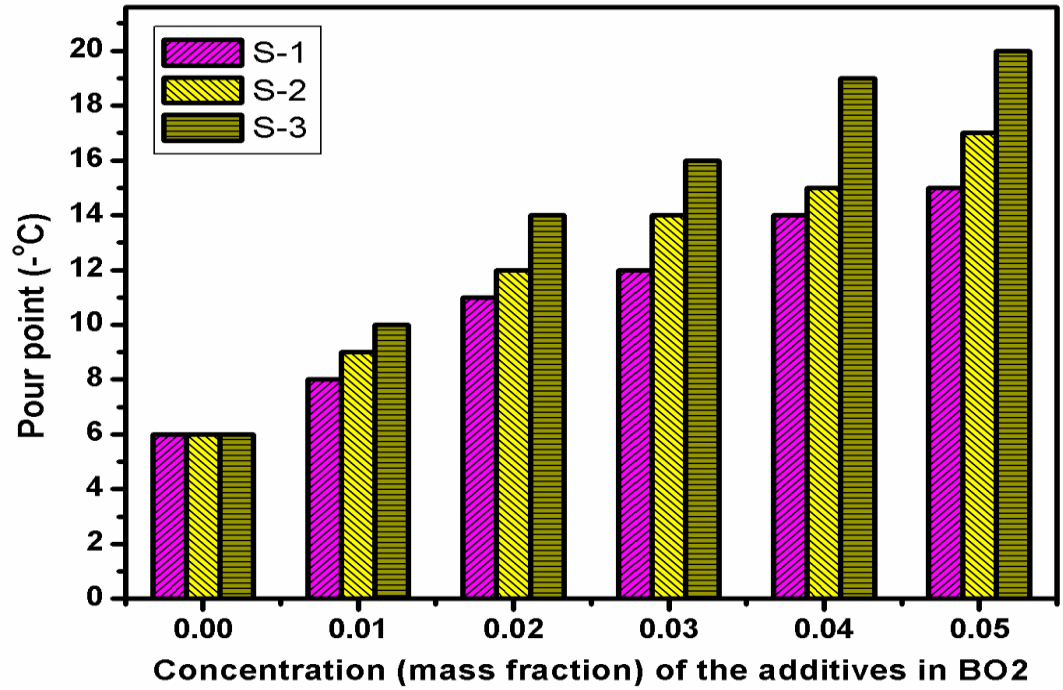

Figure 2.2.12: Photomicrographs of base oil BO1: (a) without additives (b). blended with additive S-1 at 0.03 mass fraction (c). blended with additive S-2 at 0.03 mass fraction (d). blended with additive S-3 at 0.03 mass fraction

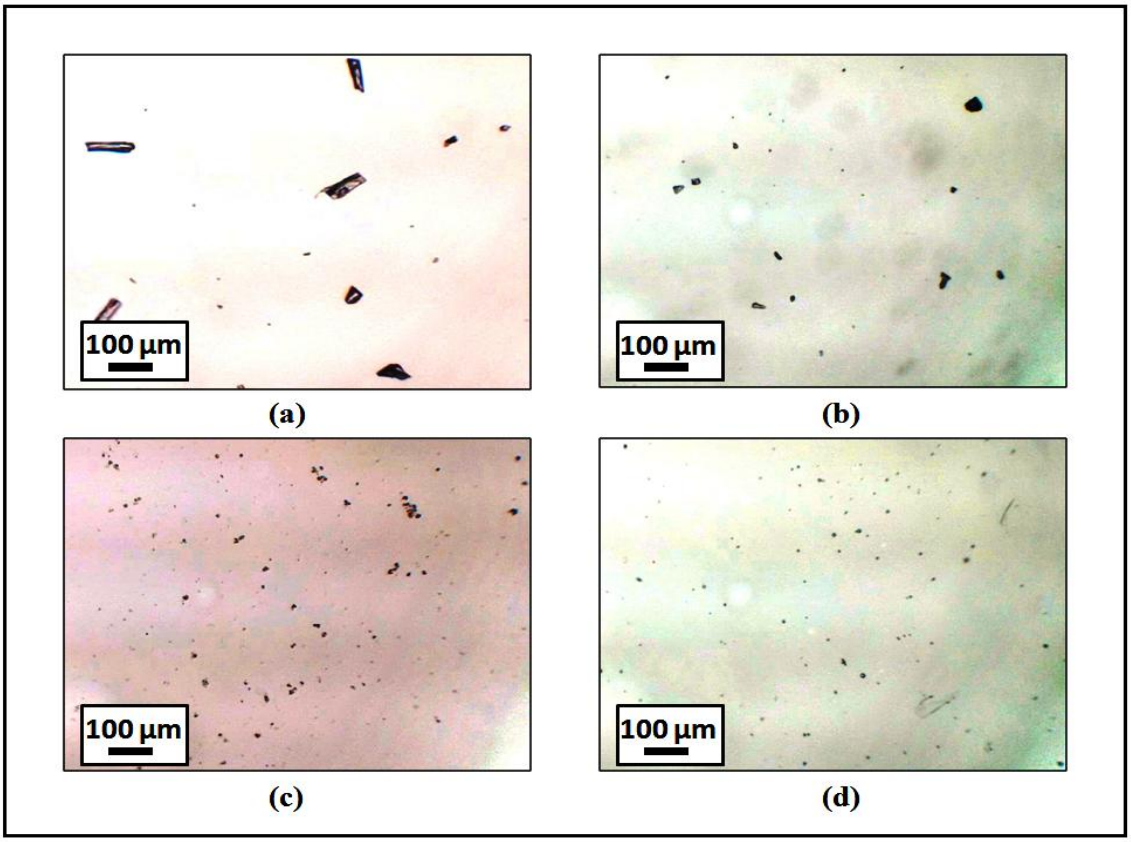

Figure 2.2.13: Degradation of almond oil (AO) and the additives measured in the SBD test